JOURNAL OF MATERIALS SCIENCE **39** (2004) 119–125

Novel pyrene and 8-anilino-1-naphthalenesulfonic acid-MoS_2 intercalates

R. BISSESSUR*, B. D. WAGNER*
Department of Chemistry, University of Prince Edward Island, Charlottetown, PEI, Canada C1A 4P3
E-mail: rabissessur@upei.ca
E-mail: bwagner@upei.ca

R. BRÜNING
Department of Physics, Mount Allison University, Sackville, New Brunswick, Canada E4L 1E6

Intercalation compounds of pyrene and 8-anilino-1-naphthalenesulfonic acid into MoS_2 have been synthesized and characterized. This was achieved by using the exfoliation/re-stacking properties of $LiMoS_2$. The degree of intercalation was found to be dependent on the amount of guest species used, the reaction time employed and the method of flocculation. The materials were also characterized by thermogravimetric analysis, four probe electrical conductivity measurements and fluorescence spectroscopy.

1. Introduction

There is significant interest in the properties of luminescent compounds due to their wide range of applications [1]. However, the luminescence quantum yield of many molecules is dramatically decreased, particularly in the solid state, because of competing non-radiative decay pathways [2]. Recently, a wide range of aromatic compounds have been shown to exhibit enhanced fluorescence when incorporated into molecular hosts such as cyclodextrins [3], cucurbiturils [4] and layered structures such as clays [5]. This enhancement in fluorescence can be ascribed to a number of factors [6], including loss of rotational freedom of the molecules and a change in the polarity of the local environment of the probe upon host inclusion. These can result in a decrease in the efficiency of radiationless transitions, and hence an increase in fluorescence, via specific mechanisms. In addition, encapsulation of the organic molecules in these hosts serves as a means of protection from quenching agents such as oxygen and other paramagnetic impurities. Pyrene and 8-anilino-1-naphthalenesulfonic acid (ANS) are two aromatic compounds that have been well studied because of their fluorescence properties. Pyrene exhibits a monomer fluorescence spectrum with well-defined vibronic bands, the relative intensity of which are dependent on the polarity of the medium [7]. Specifically, the intensity ratio of vibronic bands I and III has been shown to be directly correlated to polarity [7], and thus the fluorescence of pyrene has been widely applied as a probe of local polarity [8]. At high concentrations, pyrene exhibits excimer (excited dimer) emission, which is structureless and red-shifted relative to the monomer emission, but which can be used to indicate the interaction of neighbouring pyrene molecules in the system of interest. ANS has also been widely used as a polarity-sensitive probe. In this case, it is the fluorescence quantum yield which is highly polarity sensitive; ANS is nearly non-fluorescent in water, but shows extremely strong fluorescence in non-polar solvents [9]. Dramatic enhancement in the fluorescence of ANS has been observed when encapsulated in cyclodextrins [3b] and cucurbiturils [4].

In this article we report the inclusion of pyrene and ANS into layered molybdenum disulfide (MoS_2). MoS_2 is an interesting layered material because of its extensive use as a hydrodesulfurisation catalyst [10], solid lubricant [11] and potential application as a cathode material in lithium rechargeable batteries [12]. Intercalation compounds of MoS_2 can be achieved by using the exfoliation/re-stacking properties of Li_xMoS_2 [13]. We have exploited this synthetic methodology to intercalate pyrene and ANS into MoS_2, with the goal of using the fluorescence of these polarity-sensitive probes to characterize these materials.

2. Experimental

Pyrene (99%) and ANS (97%) (Fig. 1) were purchased from Aldrich and were used without any further purification. Li_xMoS_2 was prepared by reacting MoS_2 (99%, Aldrich) with 3 equivalents of *n*-BuLi (2.5 M solution in hexanes) in a dry box (Equation 1). The concentration of *n*-BuLi was adjusted to 1 M by adding dry pentane

*Authors to whom all correspondence should be addressed.

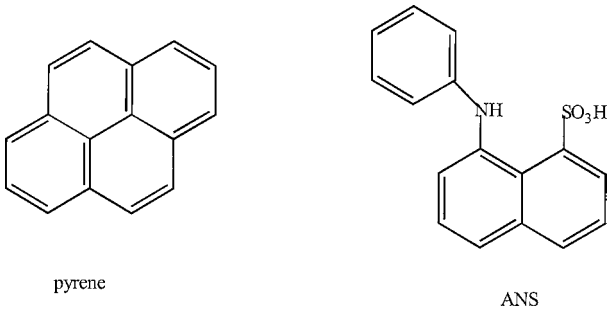

Figure 1 Structure of pyrene and ANS.

and the reaction mixture was allowed to stir for at least 2 days at room temperature. The product was filtered off in the dry box, washed with pentane and then dried under suction. Elemental analysis of the product confirmed its stoichiometry to be $LiMoS_2$. The prepared $LiMoS_2$ was stored in the dry box until future use.

$$MoS_2 + n\text{-BuLi} \rightarrow LiMoS_2 + 1/2\text{Bu-Bu} \quad (1)$$

Reaction of $LiMoS_2$ with water resulted in the formation of single layers of MoS_2 as described by Equation 2. In a typical reaction, water (20 mL) was added to $LiMoS_2$ (200 mg, 1.20 mmol) and the suspension sonicated for 2 h. This procedure resulted in complete exfoliation of the MoS_2 layers.

$$LiMoS_2 + H_2O \rightarrow (MoS_2)_{\text{single layers}} + LiOH + 1/2H_2 \quad (2)$$

A solution of pyrene in CH_2Cl_2 or ANS dissolved in ethanol was then added to the single layers and the reaction mixture was allowed to stir at room temperature for days. In some of the preparations concentrated hydrochloric acid was added after 2 days of stirring. The stirring was then further continued for several days. The reaction mixtures were then filtered off and washed thoroughly with water to remove LiOH, followed by ethanol or CH_2Cl_2 to remove excess guest species (G). This experimental procedure led to the formation of sandwiched compounds of MoS_2 as described by Equation 3.

$$(MoS_2)_{\text{single layers}} + xG \rightarrow (G)_xMoS_2 \quad (3)$$

Powder X-ray diffraction (XRD) was run on a diffractometer equipped with a graphite monochromator and an analyzer crystal was used, along with a scintillation detector. Cu K_α radiation ($\lambda = 1.542$ Å) was utilized and the data collection was carried out at 22°C. Samples were run under vacuum with a scan range of 3 to 100 degrees. In order to minimize scattering from materials other than the samples in the XRD measurements, the powdered samples were placed on a single crystal silicon substrate with the surface cut parallel to the (510) plane [supplied by The Gem Dugout, State College, PA].

Thermogravimetric analyses (TGA) were performed on a Mettler Toledo Star system using a heating rate of 10°C/min.

Electrical conductivities were measured on pressed pellets of the samples by using the conventional four probe technique. The diameter of the pellets were either 0.68 cm or 1.27 cm.

Fluorescence spectra were measured on a Photon Technology International LS-100 luminescence spectrometer using front-face emission from the solid samples. This was achieved using a 1 cm^2 solid aluminum support (the same size as a standard fluorescence cuvette used for solution work) which had been machined at a 45° angle to the excitation and emission paths of the spectrometer and painted flat black. The powder samples were directly adhered to this support using double-sided adhesive tape. The excitation wavelength used was 310 nm (pyrene) and 340 nm (ANS).

3. Results and discussion

Powder X-ray diffraction shows that we have formed genuine intercalation compounds (Fig. 2). Intercalation was found to be complete since no pristine MoS_2 phase can be observed. However, we found that the degree of intercalation depended on the amount of pyrene used in the reaction as well as on the reaction time (Table I). An increase in interlayer spacing from 1.29 Å to 1.89 Å was observed by merely increasing the reaction time for an additional 12 h. The smaller interlayer spacing values observed for these short reaction times are attributed to the phenomenon of staging similar to those observed for graphite intercalation compounds [14]. Similar trends have also been observed for the intercalation of naphthalene in MoS_2 [15]. The addition of concentrated hydrochloric acid after two days, followed by continued stirring for many days resulted in a product with a larger interlayer spacing. The maximum interlayer spacing value observed is 10.28 Å, corresponding to an inter-layer expansion of 4.13 Å (Table I). This is consistent with having the pyrene molecule lying co-planar with respect to the disulfide sheets (Fig. 3). A similar effect was observed for the ANS-MoS_2 system, showing a maximum interlayer spacing value of 11.34 Å

TABLE I Summary of results for pyrene (pyr)-MoS_2 system

Reaction time (days)	pyr:$LiMoS_2$ mole ratio	Flocculation step	Interlayer spacing (Å)	Interlayer expansion (Å)	Composition TGA in air	Crystallite size (Å)
2	0.5	No acid	7.44	1.29	$(pyr)_{0.11}(H_2O)_{0.90}MoS_2$	34
2.5	0.3	No acid	8.04	1.89	$(pyr)_{0.13}(H_2O)_{0.75}MoS_2$	34
15	5	Acid	10.16	4.01	$(pyr)_{0.18}MoS_2$	70
15	5	No acid	9.21	3.06	$(pyr)_{0.13}(H_2O)_{0.15}MoS_2$	32
22	5	Acid	10.28	4.13	$(pyr)_{0.18}MoS_2$	63

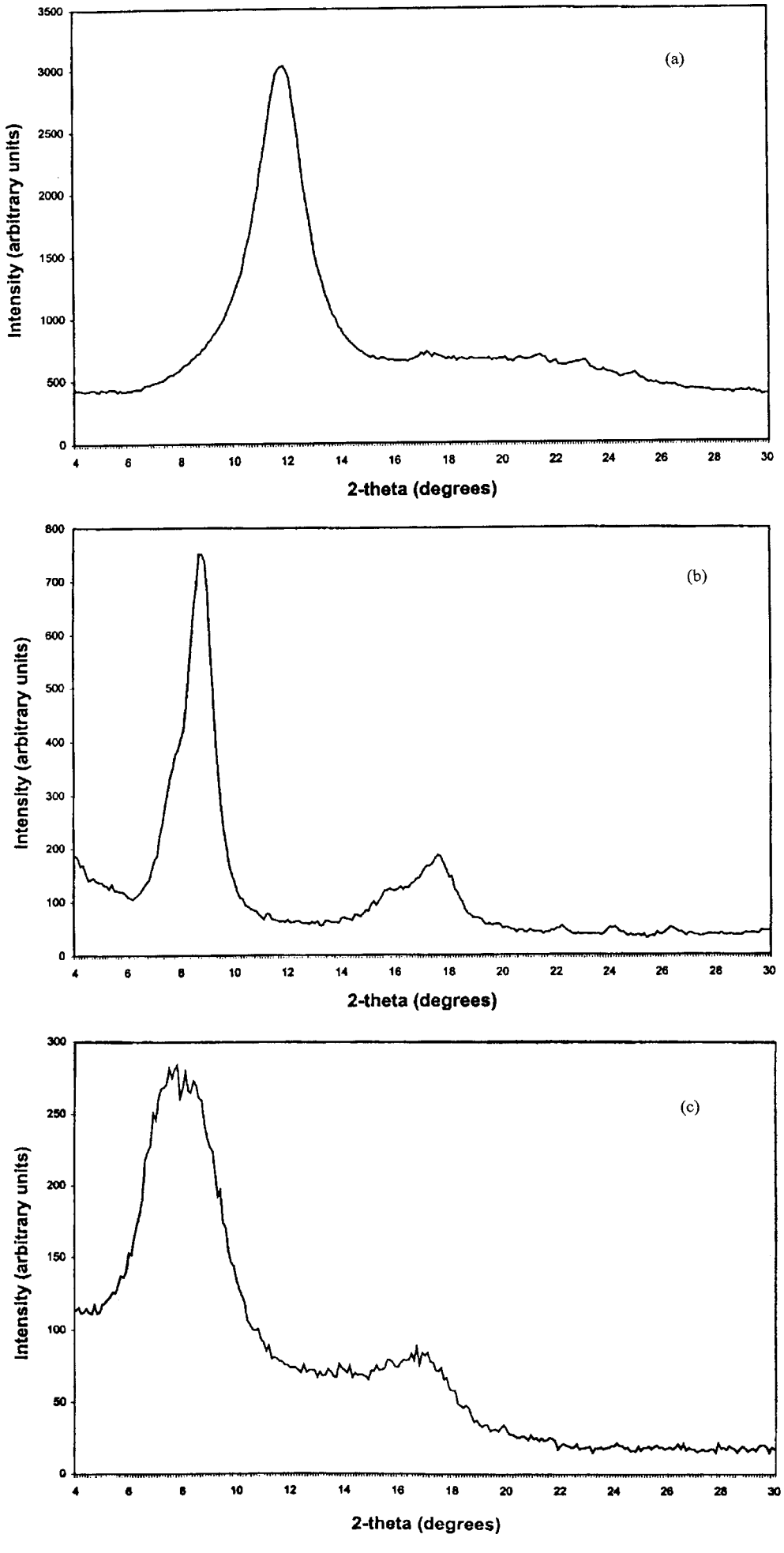

Figure 2 Powder X-ray diffraction pattern of: (a) $(pyr)_{0.11}(H_2O)_{0.90}MoS_2$, (b) $(pyr)_{0.18}MoS_2$, and (c) $(ANS)_{0.12}MoS_2$.

TABLE II Summary of results for ANS-MoS_2 system

Reaction time (days)	ANS:$LiMoS_2$ mole ratio	Flocculation step	Interlayer spacing (Å)	Interlayer expansion (Å)	Composition TA in air	Crystallite size (Å)
22	5	Acid	11.34	5.19	$(ANS)_{0.12}MoS_2$	29
22	5	No acid	10.40	4.25	$(ANS)_{0.13}MoS_2$	28

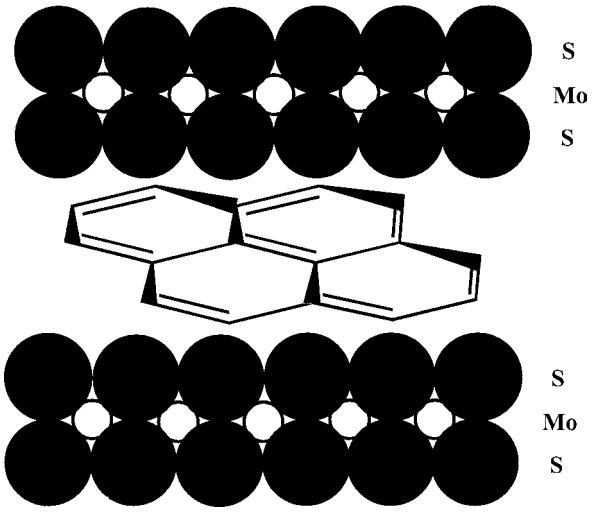

Figure 3 Schematic representation of the lamellar structure of $(pyr)_{0.18}MoS_2$.

(Table II). This slightly larger interlayer spacing value over the pyrene-MoS_2 system is consistent with the non-planar-geometry of the ANS molecule causing a slightly greater inter-layer expansion of the layered host.

The effect of the added acid on the interlayer spacing value is not well-understood. However, it is clear that the concentrated acid serves to bring the pH of the system to about 2, and shortly thereafter coagulation of the particles into a lumpy solid is observed. The acidic solution thus obtained serves as an electrolyte that helps in converting the colloidal suspension to an agglomerated form which is subsequently much easier to filter [16]. This acid treatment also helps in getting rid of loosely bound water molecules and therefore preventing their co-intercalation in between the disulfide sheets. Thermogravimetric analyses (TGA) show that materials prepared in this way do not possess any co-intercalated waters whereas omission of the acidification step results in the co-inclusion of water (*vide infra*).

The compositions of the intercalation compounds were determined by TGA under air. This method has been previously shown to give reliable results that agree closely with elemental analyses [17] and has recently been applied to macrocycles-MoS_2 intercalation compounds [18] as well as solid polymer electrolytes-MoS_2 systems [19]. For instance examination of the thermogram (Fig. 4a) for the ANS/MoS_2 system shows that the material is stable up to 275°C. Thereafter, a

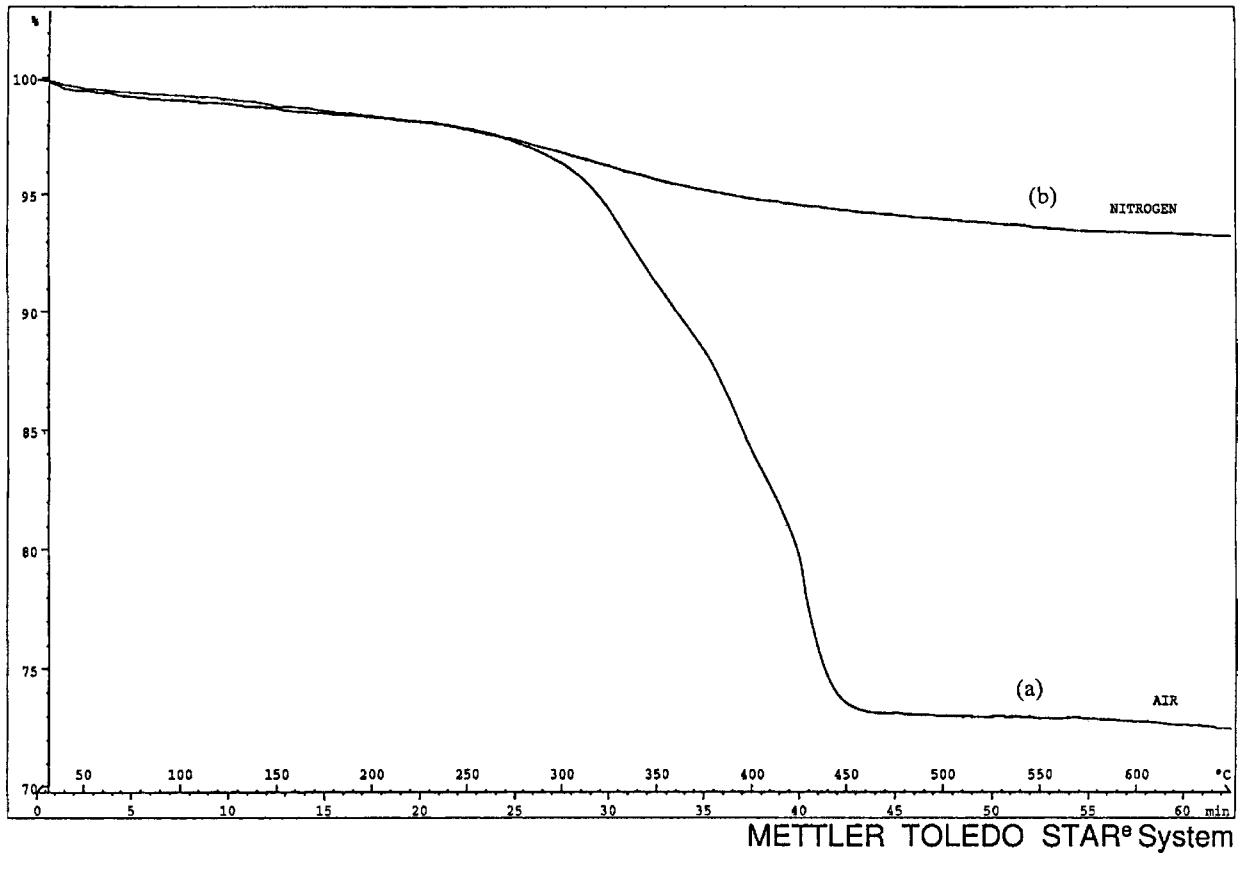

Figure 4 TGA of $(ANS)_{0.13}MoS_2$: (a) in air and (b) in nitrogen.

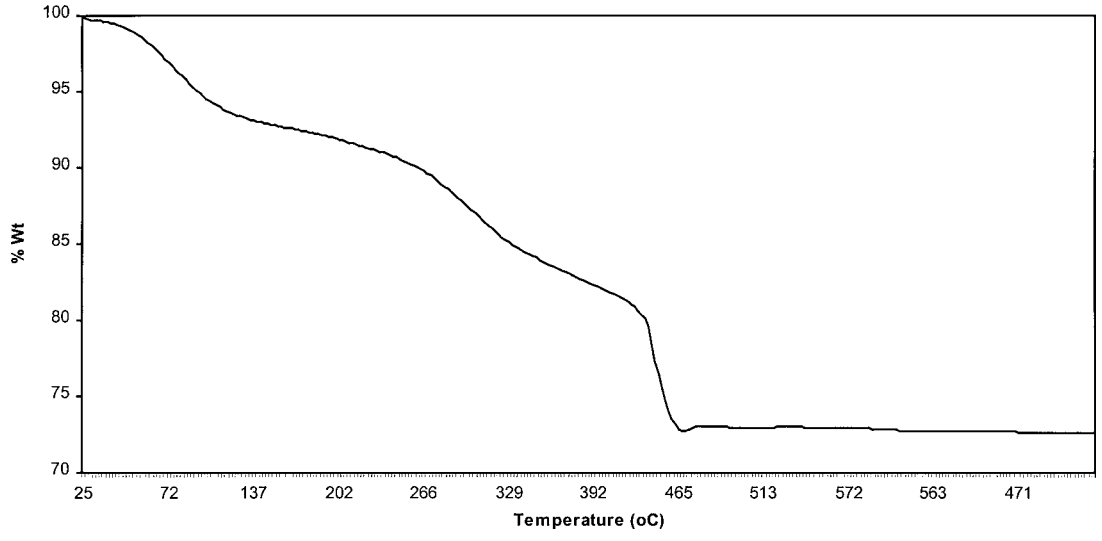

Figure 5 TGA of $(pyr)_{0.11}(H_2O)_{0.90}MoS_2$ in air.

major weight loss was observed up to 450°C, followed by the formation of MoO_3 phase which is stable up to 650°C. The identity of the MoO_3 phase was confirmed by FTIR spectroscopy and XRD. By using this information the stoichiometry of the intercalation compound was determined to be $(ANS)_{0.13}MoS_2$. The stoichiometry of the other sandwiched compounds were determined in a similar manner. However, for the intercalation of pyrene into MoS_2, co-intercalation of water molecules is observed if no acid is employed in the flocculation step. The thermograms of the resulting materials show a discernable step corresponding to the weight loss of water. For instance, the TGA (in air) of the intercalation product of pyrene (pyr) into MoS_2 (mole ratio of pyr:$LiMoS_2$:0.5, reaction time 2 days, no added acid) shows a discernable initial step corresponding to a weight loss of 8% which is attributed to the desorption of co-intercalated water molecules (Fig. 5). This step is not observable in materials prepared by the addition of acid solution. Interestingly enough, intercalation compounds of ANS in MoS_2 show no such discrete step in their thermograms, indicating that the co-inclusion of water molecules is not taking place. This is attributed to the already acidic nature of the guest species and consequently addition of an external acid source has no effect on the intercalation process. The results for the ANS/MoS_2 system are given in Table II.

The crystallite size of the intercalation compounds were determined from their powder X-ray diffraction patterns by using the Scherrer formula [20]. A simplified version of the formula is shown in Equation 4:

$$D = \frac{K * \lambda * 57.3}{\beta^{1/2} * \mathrm{Cos}\,\theta} \tag{4}$$

where D is the average crystallite size in Å, λ is the wavelength of the Cu K_α radiation (1.542 Å), $\beta^{1/2}$ is the peak width at half-height in degrees and θ is the position of the peak in degrees. K is a constant depending on the shape of the crystallites. Assuming that the crystallites are perfect spheres, K is assigned a value of 0.9. The value 57.3 is the conversion factor for radians to degrees. The crystallite size of pristine MoS_2 used in this research was calculated to have an average value of 135 Å. However, a dramatic decrease in crystallite size is observed in all the intercalation compounds. This is due to the fact that once the layers have been exfoliated they do not re-stack quite as well as in its initial state. However for the pyrene-MoS_2 system, the crystallite size of the intercalation compound doubles when concentrated HCl is added to the reaction vessel. The optimum reaction time was found to be 15 days, since stirring for a longer period of time did not lead to an increase in the crystallite size of the product. Without the addition of acid the crystallite size remains roughly the same regardless of the reaction time and the amount of pyrene used (Table I). However, for the case of ANS-MoS_2 system, the crystallite size of the intercalation compound stays the same regardless of whether acid is used or not. This is probably due to the fact that the excess ANS used in the reaction provides the acidic medium in the flocculation step and addition of an external acid solution bears no effect on the crystallite size (Table II).

The room temperature electronic conductivity of the intercalated phases was assessed by the four-probe method on pressed pellets. The measured conductivity values were 0.1 S cm^{-1}, showing an enhancement in conductivity by a factor of 20 over pristine MoS_2. The latter, which is in the 2H form, is a semiconductor with a room temperature electrical conductivity of 5×10^{-3} S cm^{-1}, as determined by the four probe technique on a pressed pellet. This dramatic increase in electrcal conductivity is explained by a structural transformation of the MoS_2 which takes place during the intercalation process. In 2H-MoS_2, the molybdenum atoms are bonded to the sulfur atoms in a trigonal prismatic arrangement. Upon treatment of 2H-MoS_2 with *n*-BuLi, reduction of the layers takes place forming $LiMoS_2$ that contains molybdenum atoms octahedrally coordinated to six sulfurs. The reaction of $LiMoS_2$ with water is fast, where oxidation of the layers results in the formation of single layers trapped in the octahedral geometry. When the single layers re-stack with the guest species sandwiched in between, the octahedral

geometry of the MoS_2 is retained. Band structure calculations by Matthesis showed that MoS_2 in the octahedral (O_h) form is metallic [21].

These compounds were also studied using fluorescence spectroscopy, however no measurable fluorescence emission (i.e., above the background signal) was obtained from either the pyrene- or the ANS-intercalation solids. This is very interesting, and is in contrast to the results we were able to obtain for other fluorescent solids under identical conditions, such as the strong, well-defined fluorescence spectrum obtained from the ANS-cucurbituril exclusion compound described in Reference [4a]. The large degree of intercalation observed via powder X-ray diffraction as described above indicates that there is a large amount of fluorescent probe present in the solids in the case of both pyrene and ANS. Thus, there must be other explanations as to the lack of fluorescence from these compounds. It is possible that the probes are present in the solids as aggregates instead of as individual molecules, and thus experience self-quenching of their fluorescence emission. However, in the case of pyrene, self-association occurring from too high a degree of loading would be expected to result in excimer emission, which is weaker and red-shifted relative to the monomer emission, but still should be relatively easy to observe. No fluorescence was recorded from either type of solid any where in the range of 350 to 600 nm, which well covers both the monomer and excimer emission range of pyrene. In the case of ANS, the presence of water would result in an extremely low fluorescence quantum yield, so it is possible that the presence of water co-included in the MoS_2 layers could result in extremely weak emission from the ANS, that we were unable to measure. However, TGA results do not support co-inclusion of water in the ANS-MoS_2 system. Furthermore, water does not have a large effect on the fluorescence quantum yield of pyrene, so the presence of water cannot explain the lack of fluorescence observed from the intercalated pyrene-MoS_2 solid.

The most likely explanation for the lack of observed fluorescence from both solids may simply be the strong absorption of the MoS_2 layers. All of these MoS_2 compounds (re-stacked[1] or intercalation) are black in colour, indicating strong absorption throughout the visible region. However, the front-face emission technique employed probes the surface of the powder, so that the excitation light needs only to pass through one layer of MoS_2 to reach the intercalated fluorescent probes. Thus, it seemed reasonable to expect that the black colour of the compound is a result of its bulk properties, and that although passing through a single MoS_2 layer might reduce the intensity of the near UV excitation light incident on the fluorescent probes, it should not completely eliminate it. However the lack of observed fluorescence, and the discounting of other explanations for this lack as outlined above, does in fact indicate that very little of the excitation light is reaching the intercalated fluorescent probes. Furthermore, any fluorescence which does occur is also being efficiently absorbed by the MoS_2 layer. While it is still possible that fluorescence from these materials might be observable using a more intense excitation source than is available in our fluorescence experiments, e.g., by laser source, or by changing the experimental set-up such that a larger area of the powder surface is probed and its emission collected, such fluorescence will be extremely weak at best.

We must conclude that these MoS_2 layers have a very high optical density in the near UV and perhaps visible regions, so high that they effectively shield incorporated molecules from incident light. Although this might have potential applications for stable materials containing light-sensitive compounds, it does mean that such materials containing absorption or fluorescence probe molecules will not function as optical or photoactive materials.

[1] Re-stacked MoS_2 is obtained by reacting $LiMoS_2$ with water and allowing the exfoliated layers to flocculate with no entrapped guest species. Re-stacked MoS_2 and pristine MoS_2 show a similar interlayer spacing value of 6.15 Å.

4. Conclusions

Intercalation compounds of the fluorescent probes pyrene and ANS into molybdenum disulfide layers were successfully prepared and characterized for the first time. Powder X-ray diffraction indicated a large increase in layer separations in the case of the intercalation compounds as compared to re-stacked MoS_2. Interesting properties of these compounds were observed, such as high electronic conductivity and high thermal stabilities. However, despite the large loading of the two different fluorescent probes into the MoS_2 layers, no fluorescence emission could be observed from these solids. This was explained to be most likely the result of the large absorption of the MoS_2 layers in the visible and UV spectral region, and indicates that these MoS_2 layers must have an exceptionally high optical density in the near UV and perhaps visible regions. These results indicate that although a wide range of intercalation compounds can be prepared from this interesting MoS_2 material, including those with incorporated fluorescent probe molecules, they will not be useful as optical materials due to the high optical density of the MoS_2 layers.

Acknowledgments

We are grateful to the Natural Sciences and Engineering Research Council (NSERC) of Canada, Canada Foundation for Innovation (CFI), Atlantic Innovation Fund of Canada (AIF) and the UPEI Senate Committee on Research for financial support.

References

1. (a) G. J. MEYER, *J. Chem. Ed.* **74** (1997) 652; (b) H. CHUANG and M. A. ARNOLD, *Anal. Chem.* **69** (1997) 1899; (c) J. N. DEMAS and B. A. DEGRAFF, *J. Chem. Ed.* **74** (1997) 690; (d) J. R. BACON and J. N. DEMAS, *Anal. Chem.* **59** (1987) 2780.
2. (a) J. B. BIRKS, in "Photophysics of Aromatic Molecules" (Wiley-Interscience, London, 1970); (b) D. C. HARRIS, in "Qualitative Chemical Analysis," 5th ed. (W. H. Freeman and Company, New York, 1999).
3. (a) R. P. FRANKEWICH, K. N. THIMMAIAH and W. L. HINZE, *Anal. Chem.* **63** (1991) 2924; (b) B. D. WAGNER and

P. J. MACDONALD, *J. Photochem. Photobiol. A: Chem.* **114** (1998) 151.
4. (a) B. D. WAGNER and A. I. MACRAE, *J. Phys. Chem.* B **103** (1999) 10114; (b) B. D. WAGNER, S. J. FITZPATRICK, M. A. GILL, A. I. MACRAE and N. STOJANOVIC, *Can. J. Chem.* **79** (2001) 1101.
5. D. W. KIM, A. BLUMSTEIN, J. KUMAR and S. K. TRIPATHY, *Chem. Mater.* **13** (2001) 243.
6. S. LI and W. C. PURDY, *Chem. Rev.* **92** (1992) 1457.
7. K. KALYANASUNDARAM and J. K. THOMAS, *J. Amer. Chem. Soc.* **99** (1977) 2039.
8. X. LIU, K.-K. IU and J. K. THOMAS, *J. Phys. Chem.* **93** (1989) 4120.
9. (a) E. M. KOSOWER, H. DODIUK and H. KANETY, *J. Amer. Chem. Soc.* **100** (1978) 4179; (b) T. W. EBBESEN and C. A. GHIRON, *J. Phys. Chem.* **93** (1989) 7139.
10. O. WEISSER and S. LANDA, in "Sulfided Catalysts: Their Properties and Applications" (Pergammon, New York, 1973).
11. P. D. FLEISCHAUER, *Thin Solid Films* **154** (1987) 309.
12. (a) C. JULIAN, S. I. SAIKH and G. A. NAZRI, *Mater. Sci. Eng.* B **15** (1992) 73; (b) H. TRIBUTSCH, *Faraday Discuss. Chem. Soc.* **70** (1980) 190; (c) F. C. LAMAN, M. W. MATSEN and J. A. R. STILES, *J. Electrochem. Soc.* (1986) 2421.
13. W. M. R. DIVIGALPITIYA, S. MORRISON and R. F. FRINDT, *Thin Solid Films* **186** (1990) 177.
14. (a) H. FUJIMOTO, A. MABUCHI, K. TOKUMITSU and T. KASUH, *Carbon* **32** (1994) 193; (b) X. QIN and G. KIRCZENOW, *Phys. Rev.* **39** (1989) 6245; (c) M. S. DRESSELHAUS and G. DRESSELHAUS, *Adv. Phys.* **30** (1981) 139; (d) X. W. QIAN and S. A. SOLIN, *Phys. Rev.* B **39** (1989) 8707; (e) S. A SOLIN and H. ZABEL, *Adv. Phys.* **37** (1988) 87.
15. L. KOSIODOWSKI and A. V. POWELL, *J. Chem. Soc. Chem. Commun.* (1998) 2201.
16. D. A. SKOOG, D. M. WEST and F. J. HOLLER, in "Fundamentals of Analytical Chemistry," 7th ed. (Saunders College Publishing, 1996).
17. R. BISSESSUR, M. G. KANATZIDIS, J. L. SCHINDLER and C. R. KANNEWURF, *J. Chem. Soc. Chem. Commun.* **20** (1993) 1582.
18. (a) R. BISSESSUR, R. I. HAINES and R. BRÜNING, *J. Mater. Chem.* **13** (2003) 44; (b) R. BISSESSUR, R. I. HAINES, D. R. HUTCHING and R. BRÜNING, *Chem. Commun.* (2001) 1598.
19. (a) R. BISSESSUR, D. GALLANT and R. BRÜNING, *Solid State Ionics* **158** (2003) 205; (b) *Idem.*, *Mater. Chem. Phys.* **82** (2003) 316; (c) *Idem.*, *J. Mater. Sci. Lett.* **22** (2003) 429.
20. P. SCHERRER, *Nachr. Ges. Wiss. Gottingen, Math.-Phys. KI.* **2** (1918) 96.
21. (a) L. F. MATTHESIS, *Phys. Rev.* **8** (1973) 3179; (b) M. A. PY and R. R. HAERING, *Can J. Phys.* **61** (1983) 76.

Received 20 March
and accepted 19 August 2003